Available online at www.sciencedirect.com
SCIENCE DIRECT®
Journal of Solid State Chemistry 177 (2004) 681–689
JOURNAL OF SOLID STATE CHEMISTRY
http://elsevier.com/locate/jssc

Effects of PAA additive and temperature on morphology of calcium carbonate particles

Jiaguo Yu,* Ming Lei, Bei Cheng, and Xiujian Zhao

State Key Laboratory of Advanced Technology for Materials Synthesis and Processing, Wuhan University of Technology, Luoshi Road 122, Wuhan 430070, PR China

Received 8 June 2003; received in revised form 10 August 2003; accepted 19 August 2003

Abstract

Calcium carbonate particles with various shapes were prepared by the reaction of sodium carbonate with calcium chloride in the absence and presence of a polyacrylic acid (PAA) at 25°C and 80°C, respectively. The as-prepared products were characterized with scanning electron microscopy and X-ray diffraction. The effects of pH, temperatures, aging time and concentration of PAA and $CaCO_3$ on the crystal form and morphologies of the as-prepared $CaCO_3$ were investigated. The results show that pH, temperatures, concentration of PAA and $CaCO_3$ are important parameters for the control of morphologies of $CaCO_3$. Various crystal morphologies of calcite, such as, plates, rhombohedras, rectangles, ellipsoids, cubes, etc. can be obtained depending on the experimental conditions. Especially, the monodispersed cubic calcite particles can be produced by PAA addition at 80°C. Moreover, higher temperature is beneficial to the formation of monodispersed cubic or rectangular calcite particles. This research may provide new insight into the control of morphologies of calcium carbonate and the biomimetic synthesis of novel inorganic materials.

Keywords: $CaCO_3$; Biomimetic synthesis; Polyacrylic acid (PAA); Temperature; Morphology; Cubic; Monodisperse

1. Introduction

The controlled synthesis of inorganic materials with specific size and morphology is an important aspect in the development of new materials in many fields such as advanced materials, catalysis, medicine, electronics, ceramics, pigments, cosmetics, etc. [1–5]. Compared with the size control, the morphology control is more demanding to achieve by means of classical procedures of colloid chemistry [5,6]. Biological systems, however, use biomacromolecules as nucleators, cooperative modifiers, and matrixes or molds to exert exquisite control over the processes of biomineralization, which result in unique inorganic–organic composites (e.g., seashells, bones, teeth, and many others) with various special morphologies and functions [7–10]. The strategy that organic additives and/or templates are used to control the nucleation, growth, and alignment of inorganic particles has been universally applied for the biomimetic synthesis of inorganic materials with unusual and complex form [11,12].

The biomimetic synthesis of calcium carbonate ($CaCO_3$), one of the most abundant biominerals, has received much attention owing to its wide application in such industrial fields as paper, rubber, plastics, paint, etc. [13]. The application of $CaCO_3$ particles is determined by a number of strictly defined parameters, such as morphology, structure, size, specific surface area, brightness, oil adsorption, chemical purity, and so on. One of the most important parameters is particle morphology. Therefore, the control of crystal shape and size is fundamental from the viewpoint of technical application. Among more than 60 known biominerals, the two polymorphs of $CaCO_3$, calcite and aragonite, are by far the most common, whereas vaterite, a less stable polymorph, is not commonly formed by organisms [11,12]. Biomimetic synthesis of $CaCO_3$ crystals in the presence of organic templates and/or additives has been intensively investigated in recent years. Langmuir monolayers [14–16], self-assembled monolayers (SAMs) [17–19], crystal-imprinted polymer surfaces [20], and crosslinked gelatin films [21,22] have been used as templates or matrices for the controlled growth of $CaCO_3$ crystals. Moreover, a variety of macromolecular additives, including biomacromolecules [23,24], a

*Corresponding author. Fax: +86-2787883610.
E-mail address: yujiaguo@public.wh.hb.cn (J. Yu).

0022-4596/$ - see front matter © 2003 Elsevier Inc. All rights reserved.
doi:10.1016/j.jssc.2003.08.017

designed peptide [25], and dendrimers [26,27], have exhibited obvious influences on the crystallization of $CaCO_3$. The biomimetic synthesis of $CaCO_3$ thin films has been achieved by using the cooperative effect of organic substrates and soluble polymeric additives [28,29]. Furthermore, emulsion foams [30], water-in-oil microemulsions [31], pseudovesicular double emulsions [32], and gold colloids [33] have been used as templates to achieve the morphogenesis of $CaCO_3$ with complex morphologies. Recently, the double-hydrophilic block copolymers (DHBC) have been used as a new additive for the effective control of the morphology of $CaCO_3$ [5,9]. These polymers consist of one hydrophilic block designed to interact strongly with the appropriate inorganic minerals and surfaces, and another hydrophilic block that does not interact (or only weakly) with mineral surfaces and mainly promotes solubilization in water. Owing to the separation of the binding and the solvating moieties, these polymers turned out to be extraordinarily effective in crystallization control for various inorganic materials [5].

In this work, we studied the crystallization of $CaCO_3$ particles from aqueous solutions in the absence and presence of polyacrylic acid (PAA). The effects of experimental conditions including pH, temperatures, aging time, concentration of PAA and $CaCO_3$ on the crystal form and morphologies of the as-prepared $CaCO_3$ were investigated and discussed. Calcite with different shapes was obtained. The monodispersed cubic micron-sized calcium carbonate particles were prepared by the reaction of sodium carbonate with calcium chloride at the presence of PAA at 80°C, for the first time.

2. Experimental

2.1. Preparation

PAA was obtained from Jiangshu Huarun Chemical Factory (China). The average molecular weight M_W and M_n are ca. 300,000 and ca. 100,000, respectively. All chemicals were of A.R. grade and used without further purification. Distilled water was used in this work. The precipitation of $CaCO_3$ was carried out in glass beakers at different temperature according to the method reported by literatures [5,9], respectively. Aqueous solutions of Na_2CO_3 (0.5 M) and of $CaCl_2$ (0.5 M) were first prepared as stock solutions. In a typical synthesis, a solution of Na_2CO_3 (0.5 M, 1.28 mL) was injected into an aqueous solution of PAA (80 mL, 1.0 g/L) and the pH of the solution was adjusted to a desired pH (e.g., pH 10) by using HCl or NaOH. Then a solution of $CaCl_2$ (0.5 M, 1.28 mL) was injected quickly into the pH-adjusted solution under vigorous stirring by using a magnetic stirrer. The mixture was stirred for 1 min, and then the solution kept under static conditions for 24 h (unless otherwise specified) before the product was collected for characterization. In the experiments, the starting pH was varied from 12 to 9, the concentration of PAA was varied from 5 to 0.2 g/L, the final concentration of $CaCO_3$ was varied from 32 to 4 mM, and the temperatures of the solution were kept at 25°C and 80°C, respectively. As reference experiments, the $CaCO_3$ precipitates were also prepared in the absence of PAA, and all the other conditions kept the same.

2.2. Characterization

The resulting $CaCO_3$ precipitates were characterized by scanning electron microscopy (SEM) (type JSM-5610LV) with an accelerating voltage of 20 kV. The powder X-ray diffraction (XRD) patterns were obtained on a Philips MPD 18801 X-ray diffractometer using Cu$K\alpha$ radiation at a scan rate of 0.05° $2\theta\,S^{-1}$. The accelerating voltage and the applied current are 35 kV and 20 mA, respectively.

3. Results and discussion

Fig. 1(a) and (b) show SEM micrographs of $CaCO_3$ particles obtained at 25°C and 80°C under the standard synthesis condition, respectively. At 25°C, the $CaCO_3$ aggregate particles of regular plate-like were produced

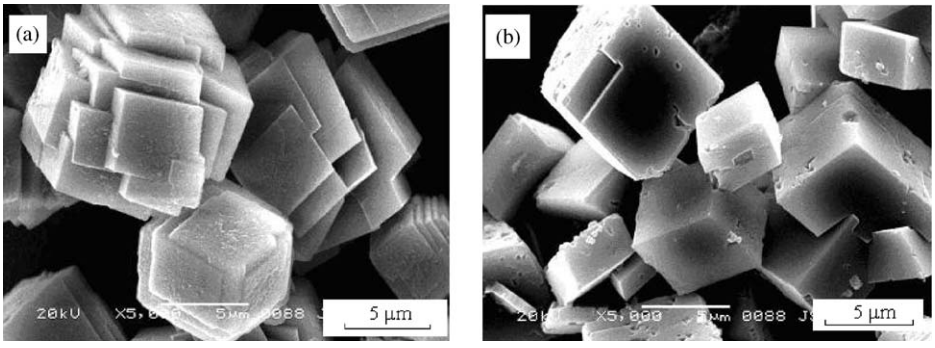

Fig. 1. SEM micrographs of $CaCO_3$ particles obtained at 25°C (a) and 80°C (b). [$CaCO_3$]: 8 mM, pH: 10.

and the particle size is about 6–12 μm. The XRD results show that the phase structure is calcite (Fig. 2(a)). At 80°C, the shapes of $CaCO_3$ particles appear as a mixture of rhombohedra and rectangle. The particle size slightly becomes small. The corresponding XRD result suggests that the crystal form is also calcite.

3.1. Effect of the polymer concentration

Fig. 3 shows the influence of the amount of PAA on morphologies of $CaCO_3$ particles at 25°C under the standard synthesis condition. When the amount of PAA is small, well-defined rhombohedral and rectangular crystals were obtained. This may be ascribed to the fact that the concentration of PAA is too low to bind enough calcium ions. However, when the amount of PAA becomes larger (from 1.0 to 2.0 g/L), large irregular-shaped round particles were obtained (Fig. 3(c) and (d)), typical for the strong interaction between the carboxylic acid groups of PAA and the crystallizing $CaCO_3$, which effectively suppresses crystal growth [5]. When the concentration of PAA reaches 5 g/L, the obtained $CaCO_3$ crystals exhibit a twinned morphology with smooth surfaces (Fig. 3(e)). A groove could be seen at the equator of the spheres, almost separating them into two halves. The occurrence of these equators could be explained if the spheres were formed via a sheaf-of-wheat mechanism as described in Ref. [35]. The equator would be due to the meeting of the opposite ends of sheafs. The corresponding XRD result (Fig. 2(b)) shows that these irregular-shaped twinned ellipsoidal particles are composed of calcite with a size of about 50 nm, as determined by (104) diffraction peak according to the Scherrer equation. These results are also basically consistent with the crystallization of $CaCO_3$ in the presence of PMAA [5,34].

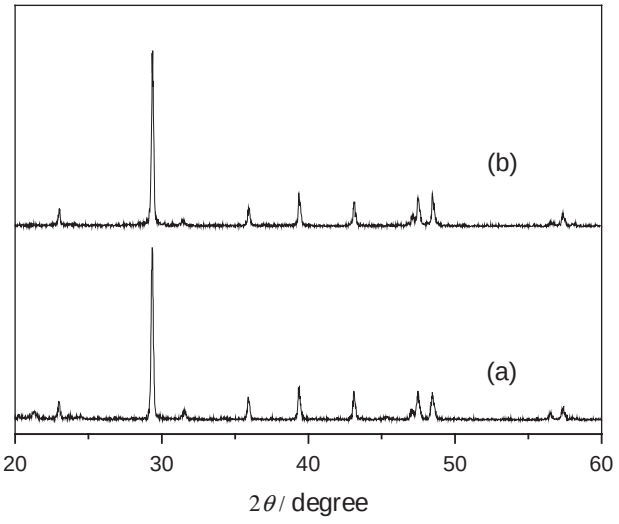

Fig. 2. XRD patterns of $CaCO_3$ particles obtained in the presence of no PAA (a) and PAA (b) at 25°C. [$CaCO_3$]: 8 mM, pH: 10; [polymer]: 5.0 g/L.

Fig. 4 shows the influence of the concentration of PAA on morphologies of $CaCO_3$ particles at 80°C. At PAA concentration of 0.2 g/L, rod-like or branched irregular particles with rugged and faceted surfaces were produced. Meanwhile, small rhombohedral and cubic crystals (1–5 μm) in addition to the rugged species were also obtained. This suggests that the presence of a small amount of PAA has obvious influence on the crystal morphology at 80°C. With the increasing of the amount of PAA, irregular rod-like or branched particles gradually disappeared (Fig. 4(b)). When the concentration of PAA reaches 1.0 g/L, the monodispersed cubic calcite particles were produced. When the concentration of PAA reaches 5.0 g/L, the obtained $CaCO_3$ crystals exhibit aggregates of micro-size cubes and cubes gradually becomes round. By comparing Figs. 3 and 4, it can be found that high temperature is more beneficial to the formation of monodispersed cubic calcite particles. This may provide new insight into the control of morphologies of calcium carbonate.

$CaCO_3$ particles in cube shape are desirable in such industries as the papermaking and the paint making. As filler or a reinforcing material, the cubic calcite particles may confer high smoothness and excellent gloss to the composite since they are easily aligned in a regular way. They may also confer high electric resistance and elasticity modulus to the composite.

In order to further investigate the formation process of the monodispersed cubic calcite particles (Fig. 4(c) and (d)), we tried to follow the morphological development of the cubic calcite particles at different crystallization times. Fig. 5 shows typical SEM micrographs of $CaCO_3$ particles obtained in the presence of PAA at 80°C after different aging time. It can be seen from Fig. 5(a) that at the early stages large cubic species (about 3 μm) are formed. These big particles resemble in shape and size the cubic calcite particles aged for 12 and 24 h shown in Fig. 5(b) and (c), that is, the particles do not further grow in the remaining time of the reaction. This means that the crystallization of calcite is completed at early stage. With increasing aging time, the sizes of calcite particles almost become the same size due to Ostwald ripening, and the size distribution of calcite particles becomes monodisperse after 24 h.

Fig. 6 shows the effect of aging time on morphologies of $CaCO_3$ particles obtained in the presence of PAA at 25°C. At the early stages, large spherical species (about 3 μm) are formed. With increasing aging time, the particles become more round and the particle size slightly increases.

3.2. Effect of pH

The variation of pH obviously influences the morphology of the produced $CaCO_3$ crystals, although the XRD results suggest that all of the products are calcite

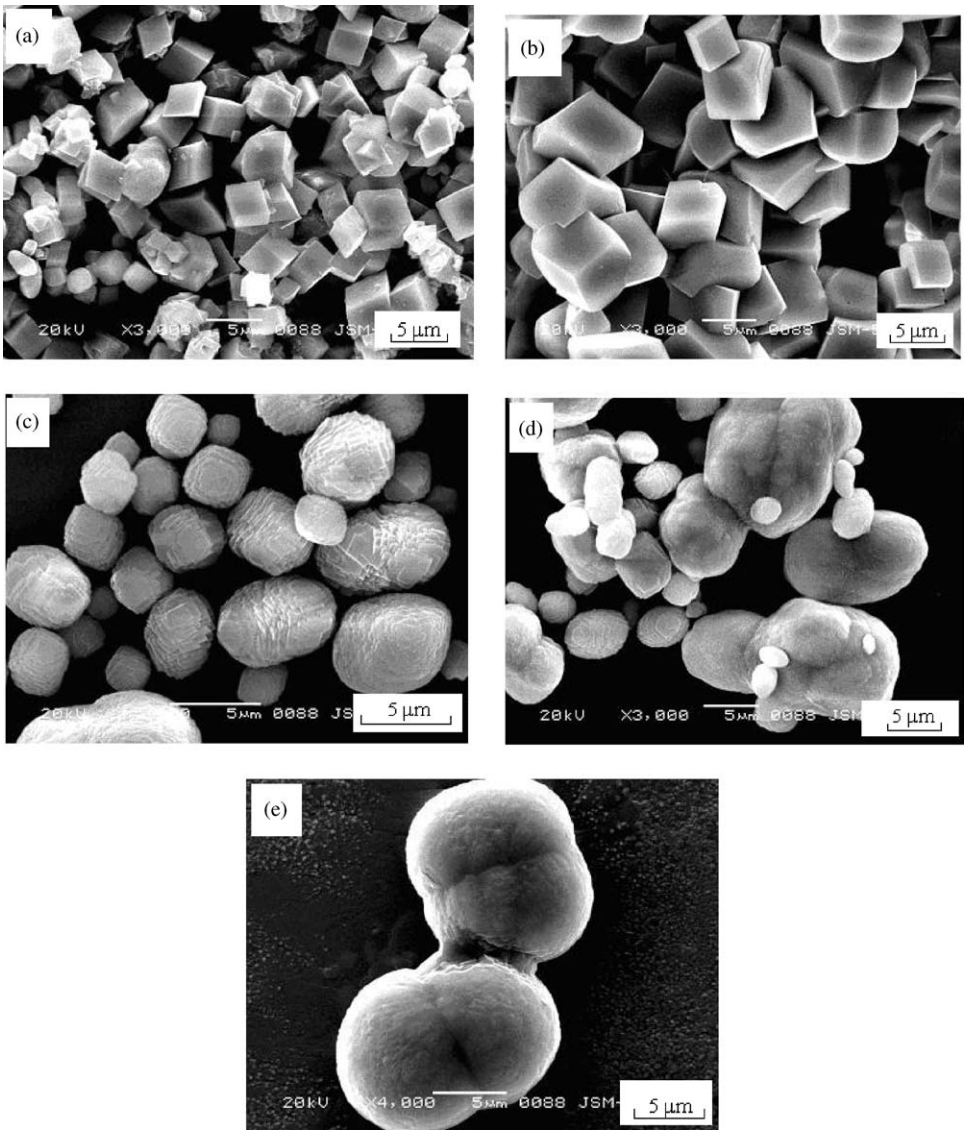

Fig. 3. SEM micrographs of $CaCO_3$ particles obtained in the presence of PAA at 25°C. [$CaCO_3$]: 8 mM, pH: 10; [PAA]: (a) 0.2, (b) 0.5, (c) 1.0, (d) 2.0 and (e) 5.0 g/L.

crystals. Fig. 7 shows the SEM pictures of the products obtained at various pH at 25°C. Uniform plate-like aggregate particles with a size of 4–8 μm were obtained by decreasing the pH from 10 to 9. The increase of pH from 10 to 11 and 12 resulted in the formation of round and irregular aggregate particles. At pH 12, the aggregation of particles was greatly enhanced. It is observed that the particle size is at a maximum at pH 9, that is, the nucleation rate is lowest at the lowest pH. This may be related to the influence of pH on the protonation degree of the carboxylic acid groups in PAA. In the pH range 9–12, the carboxylic acid groups are completely charged and form a polyanionic chain [5]. The remaining minor difference in protonation is presumably not relevant for changing the rate of nucleation. On the other hand, the solution supersaturation increases with increasing pH, which is due to the hydrocarbonate/carbonate buffer equilibrium, coupled with an increasing nucleation rate of $CaCO_3$ [5]. The nucleation rate at high pH, such as 11 and 12, is so high that morphology control is already partially lost and the particle size slightly decreases. This is due to the fact that precipitation takes place immediately at high pH, whereas with decreasing pH the induction time of $CaCO_3$ precipitation increased considerably [5]. This also shows the decrease of the supersaturation making the crystallization control by the polymer more efficient.

Fig. 8 shows that the influence of pH on the morphologies of $CaCO_3$ particles obtained in the presence of PAA at 80°C. At low pH values (9–11), the pH has no obvious influence on the morphology of cubic $CaCO_3$ particles. At pH 12, smaller irregular aggregate particles were obtained.

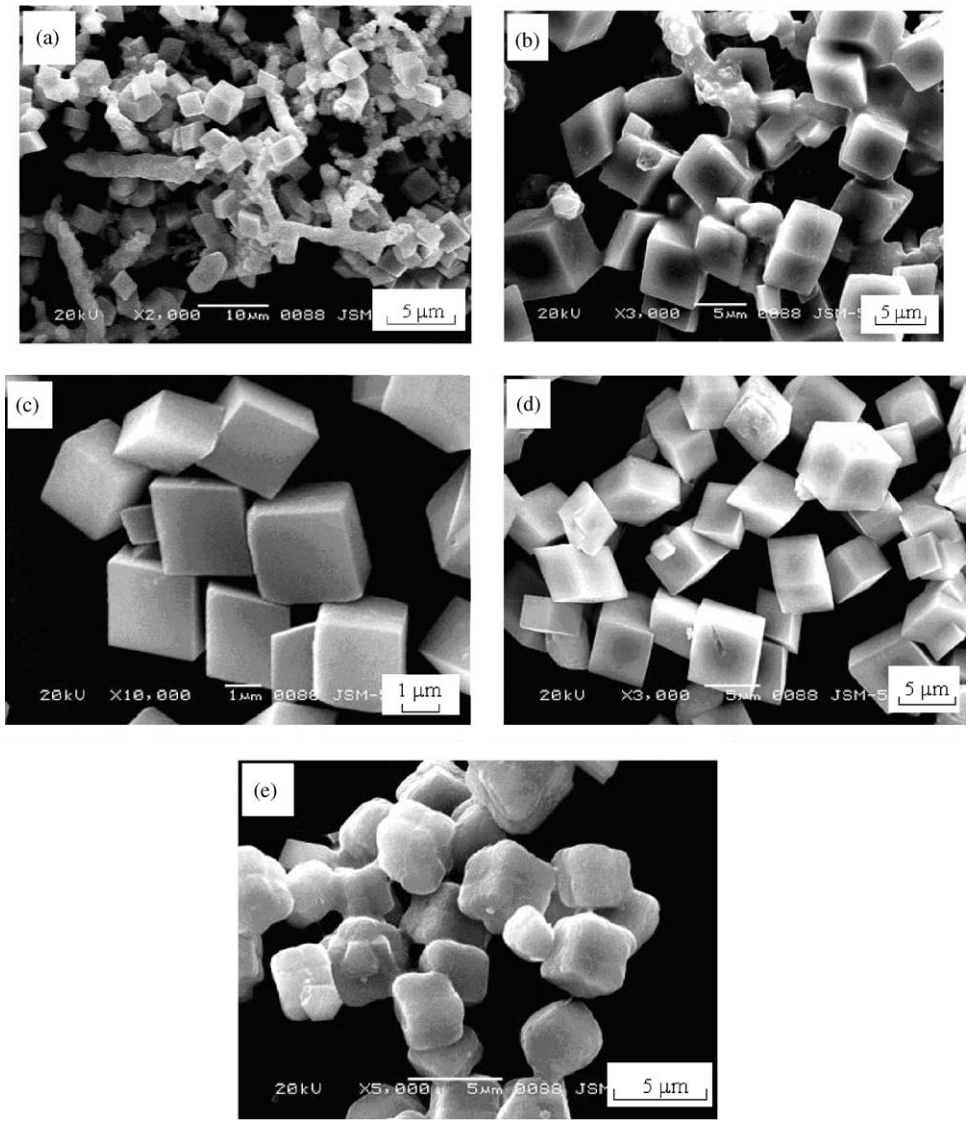

Fig. 4. SEM micrographs of $CaCO_3$ particles obtained in the presence of PAA at 80°C. [$CaCO_3$]: 8 mM, pH: 10; [PAA]: (a) 0.2, (b) 0.5, (c) 1.0, (d) 2.0 and (e) 5.0 g/L.

3.3. *Effect of the $CaCO_3$ concentration*

To examine the influence of the $CaCO_3$ concentration on the crystallization, the crystallization experiment was carried out at $CaCO_3$ concentrations of 4, 16 and 32 mM at 25°C and 80°C. XRD results show that all the samples are composed of calcite and the $CaCO_3$ concentration has no influence on the phase structure.

Fig. 9 shows that the influence of the $CaCO_3$ concentration on the morphologies of $CaCO_3$ particles obtained in the presence of PAA at 25°C. At the $CaCO_3$ concentration of 4 mm, the ellipsoidal and irregular particles were obtained, same as those in Fig. 3(d). This is attributed to the increase in the relative ratio of polymer to $CaCO_3$. Decreasing the $CaCO_3$ concentration has a similar result as increasing the concentration of polymer. If the $CaCO_3$ concentration was increased to 16 and 32 mM, a mixture of plate-like and less-defined calcite particles were obtained, same as those in Figs. 3(a) and (b). Both $CaCO_3$ concentration experiments indicate that the relative proportion between the polymer and $CaCO_3$ concentrations is more relevant for determining the morphology of the produced particles. A similar trend can also be observed at 80°C (as shown in Fig. 10).

4. Conclusions

The pH, temperatures, concentration of PAA and $CaCO_3$ turned out to be important parameters for the control of morphologies of $CaCO_3$. Various crystal morphologies of calcite, such as plates, rhombohedras, rectangles, ellipsoids, cubes, etc. can be obtained by

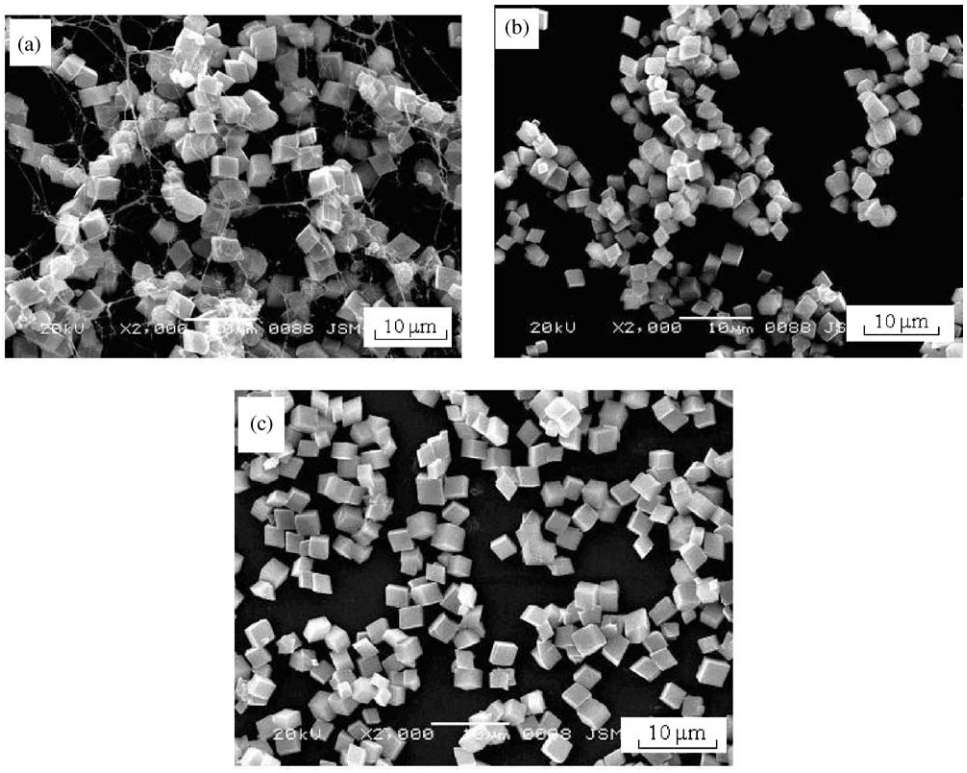

Fig. 5. SEM micrographs of $CaCO_3$ particles obtained in the presence of PAA at 80°C after (a) 2, (b) 12 and (c) 24 h. [CaCO3]: 8 mM, pH: 10; [polymer]: 1.0 g/L.

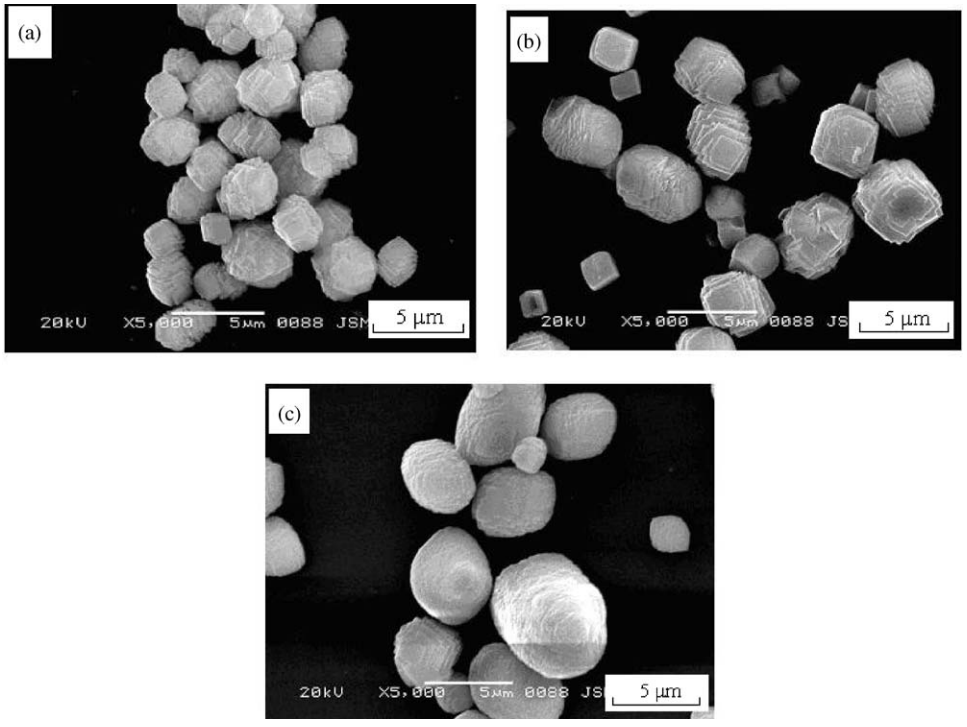

Fig. 6. SEM micrographs of $CaCO_3$ particles obtained in the presence of PAA at 25°C after (a) 2, (b) 12 and (c) 24 h. [CaCO3]: 8 mM, pH: 10; [polymer]: 1.0 g/L.

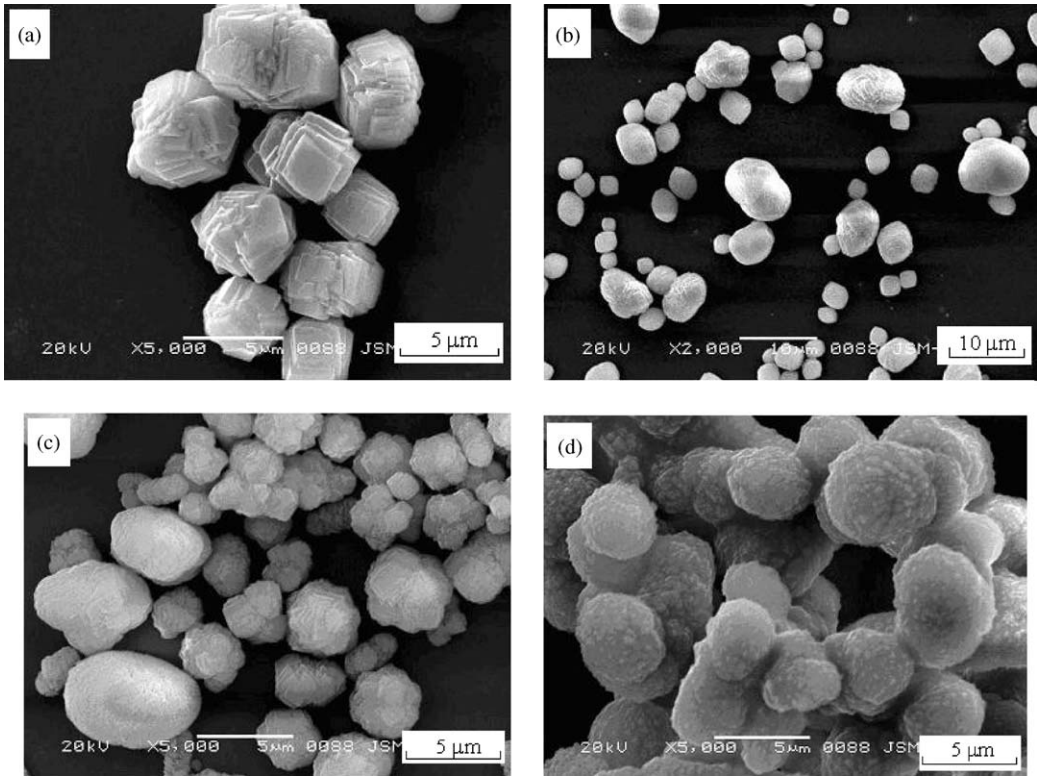

Fig. 7. SEM micrographs of $CaCO_3$ particles obtained in the presence of PAA at 25°C after 24 h. [$CaCO_3$]: 8 mM; [polymer]: 1.0 g/L, pH: (a) 9, (b) 10, (c) 11 and (d) 12.

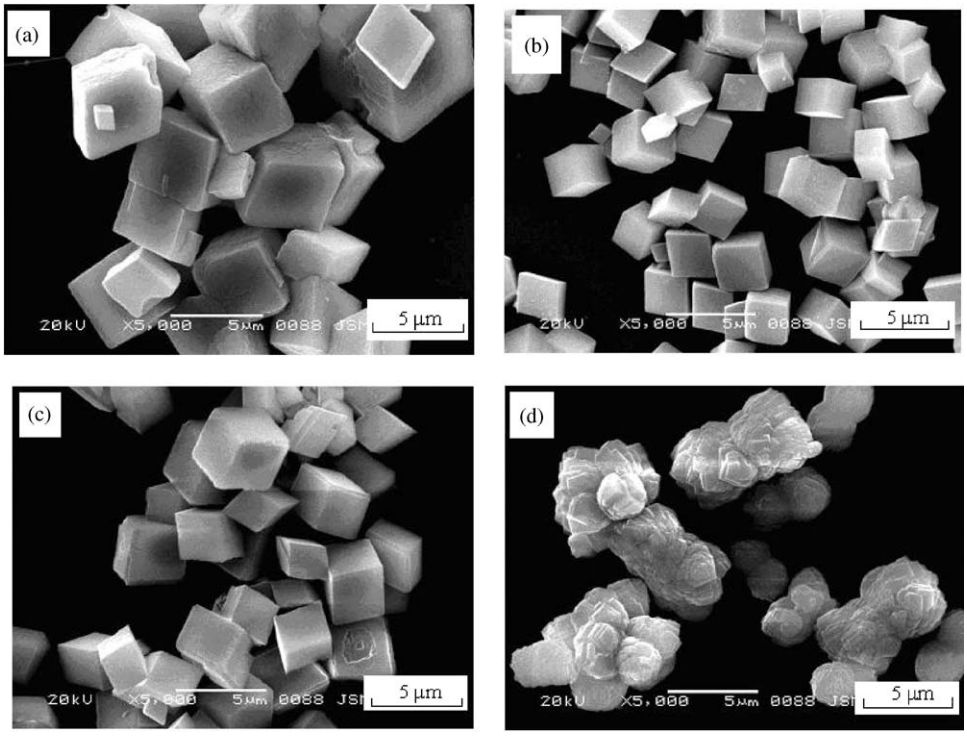

Fig. 8. SEM micrographs of $CaCO_3$ particles obtained in the presence of PAA at 80°C after 24 h. [$CaCO_3$]: 8 mM; [polymer]: 1.0 g/L, pH: (a) 9, (b) 10, (c) 11 and (d) 12.

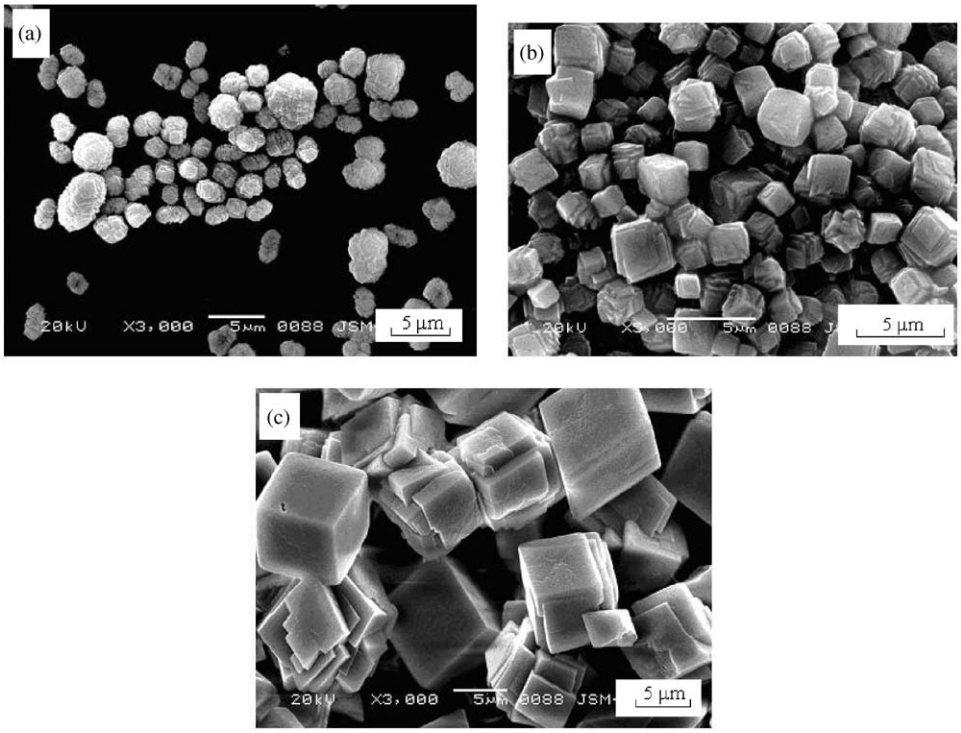

Fig. 9. SEM micrographs of $CaCO_3$ particles obtained in the presence of PAA at 25°C after 24 h. [$CaCO_3$]: (a) 4, (b) 16, (c) 32; [polymer]: 1.0 g/L, pH: 10.

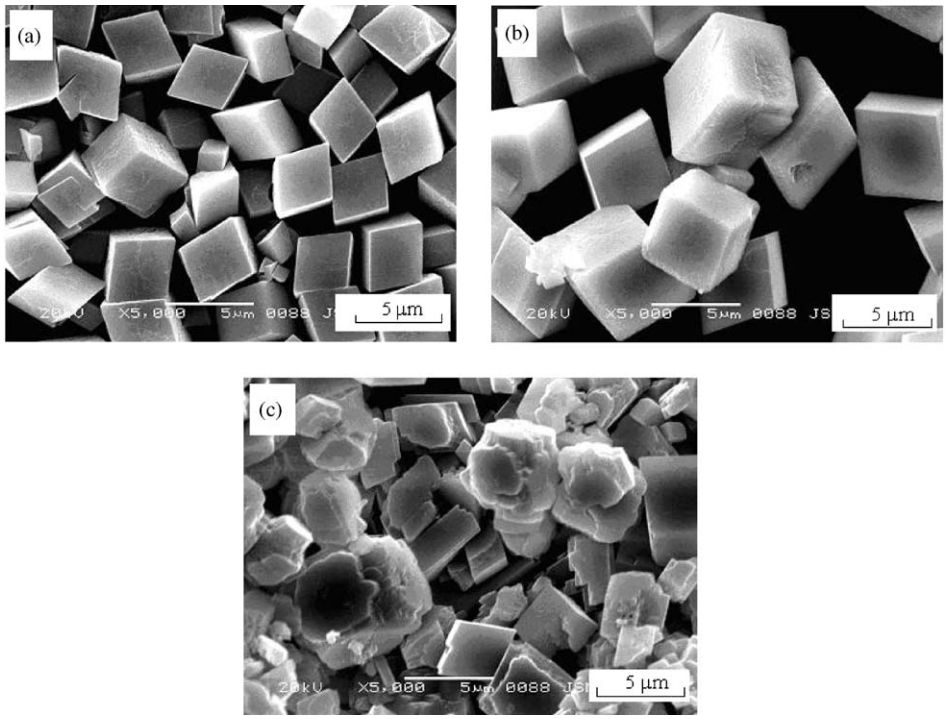

Fig. 10. SEM micrographs of $CaCO_3$ particles obtained in the presence of PAA at 80°C after 24 h. [$CaCO_3$]: (a) 4, (b) 16, (c) 32; [polymer]: 1.0 g/L, pH: 10.

changing the experimental conditions. The monodispersed cubic calcite particles can be produced by PAA as additive at 80°C. Higher temperature is more beneficial to the formation of monodispersed cubic calcite particles.

Acknowledgments

This work was partially supported by the National Natural Science Foundation of China (50272049). This work was also financially supported by the Excellent Young Teachers Program of MOE of China and Project-Sponsored by SRF for ROCS of SEM of China.

References

[1] S. Mann, G.A. Ozin, Nature 382 (1996) 313.
[2] H. Yang, N. Coombs, G.A. Ozin, Nature 386 (1997) 692.
[3] T.S. Ahmadi, Z.L. Wang, T.C. Green, A. Henglein, M.A. El-Sayed, Science 272 (1996) 1924.
[4] E. Matijevic, Curr. Opin. Colloid Interface Sci. 1 (1996) 176.
[5] H. Colfen, L. Qi, Chem. Eur. J. 7 (2001) 106.
[6] S. Mann, J. Webb, R.J.P. Williams, Biomineralization, Chemical and Biochemical Perspectives, VCH, Weinheim, 1989.
[7] S. Mann, Nature 365 (1993) 499.
[8] S. Mann, Biomimetic Materials Chemistry, VCH, Weinheim, 1995.
[9] L. Qi, J. Li, J. Ma, Adv. Mater. 14 (2002) 300.
[10] L. Qi, H. Colfen, M. Antonietti, Chem. Mater. 12 (2000) 2392.
[11] G. Falini, S. Albeck, S. Weiner, L. Addadi, Science 271 (1996) 67.
[12] D.B. DeOliveira, R.A. Laursen, J. Am. Chem. Soc. 119 (1997) 10627.
[13] E. Dalas, P. Klepetsanis, P.G. Koutsoukos, Langmuir 15 (1999) 8322.
[14] S. Mann, B.R. Heywood, S. Rajam, S.J.D. Birchall, Nature 334 (1988) 692.
[15] J.M. Didymus, S. Mann, W.J. Benton, I.R. Collins, Langmuir 11 (1995) 3130.
[16] A.L. Litvin, S. Valiyaveettil, D.L. Kaplan, S. Mann, Adv. Mater. 9 (1997) 124.
[17] J. Kuther, G. Nelles, R. Seshadri, M. Schaub, H.J. Butt, W. Tremel, Chem. Eur. J. 4 (1998) 1834.
[18] J. Aizenberg, A.J. Black, G.M. Whitesides, Nature 398 (1999) 495.
[19] J. Aizenberg, A.J. Black, G.M. Whitesides, J. Am. Chem. Soc. 121 (1999) 4500.
[20] S.M. D'Souza, C. Alexander, S.W. Carr, A.M. Waller, M.J. Whitcombe, E.N. Vulfson, Nature 398 (1999) 312.
[21] G. Falini, S. Fermani, M. Gazzano, A. Ripamonti, Chem. Eur. J. 3 (1997) 1807.
[22] G. Falini, S. Fermani, M. Gazzano, A. Ripamonti, Chem. Eur. J. 4 (1998) 1048.
[23] A.M. Belcher, X.H. Wu, R.J. Christensen, P.K. Hansma, G.D. Stucky, D.E. Morse, Nature 381 (1996) 56.
[24] G. Falini, S. Albeck, S. Weiner, L. Addadi, Science 271 (1996) 67.
[25] D.B. DeOliveira, R.A. Laursen, J. Am. Chem. Soc. 119 (1997) 10627.
[26] K. Naka, Y. Tanaka, Y. Chujo, Y. Ito, Chem. Commun. (1999) 1931.
[27] J. Donners, B.R. Heywood, E. Meijer, R. Nolte, C. Roman, A. Schenning, N. Sommerdijk, Chem. Commun. (2000) 1937.
[28] G. Xu, N. Yao, I.A. Aksay, J.T. Groves, J. Am. Chem. Soc. 120 (1998) 11977.
[29] A. Sugawara, T. Kato, Chem. Commun. (2000) 487.
[30] D. Walsh, S. Mann, Nature 377 (1995) 320.
[31] D. Walsh, B. Lebeau, S. Mann, Adv. Mater. 11 (1999) 324.
[32] T. Hirai, S. Hariguchi, I. Komasawa, R.J. Davey, Langmuir 13 (1997) 6650.
[33] J. Kuther, R. Seshadri, G. Nelles, W. Assenmacher, H.J. Butt, W. Mader, W. Tremel, Chem. Mater. 11 (1999) 1317.
[34] J.M. Marentette, J. Norwig, E. Stockelmann, W.H. Meyer, G. Wegner, Adv. Mater. 9 (1997) 647.
[35] R.B. Williamson, J. Crystal Growth 3–4 (1968) 787.